Supplementary Material

This supplement contains additional analyses and description of methods to supplement the main manuscript. Additional references cited only within this supplemental document are listed at the end.

S1 Comparison of ERA5-Land with Test Reference Years (TRY) data set

In order to put the partially large deviations between the NUKLEUS simulations and ERA5-Land into context, we here compare ERA5-Land for the historical reference period 1961–1990 used in this study and the data for the evaluation period 2005–2014 used in Sieck et al. (2026) with the Test Reference Years (TRY) data set (Krähenmann et al., 2016). TRY is a gridded observation-based data set for Germany provided by Germany's National Meteorological Service (DWD) with a high spatial resolution of $1\,\mathrm{km} \times 1\,\mathrm{km}$ and hourly temporal resolution for the period 1995–2012. The gridded data is derived using ground-based synoptic stations and additional supporting information from CM-SAF satellite observations and COSMO-CLM model data. Therefore, TRY is expected to represent the actual climatic conditions more accurately than ERA5-Land, especially in regions with characteristic geographic features, such as complex orography or coastal regions.

The quality assessment is done comparing the diurnal cycles of ERA5-Land (both periods) and TRY for entire Germany and the two pilot regions of EF and PAR, which exhibit the two orographic extremes of flat coastal (EF) and complex mountainous (Pre-)Alpine areas. All data sets are interpolated to and analyzed on the NUKLEUS CEU-3 grid.

Figure S1 shows the diurnal cycles of $2\,\mathrm{m}$ temperature. The ERA5-Land data during the evaluation period shows a high agreement with TRY for entire Germany and the flat EF region, with only small deviations of less than $0.2\,\mathrm{K}$. In the mountainous PAR region, the deviations are larger, especially during nighttimes, with up to $2\,\mathrm{K}$. The ERA5-Land data for the historical reference period is about $1\,\mathrm{K}$ lower throughout the entire day, which aligns well with the climate change-related warming rate between the two periods for Germany stated by DWD (2026).

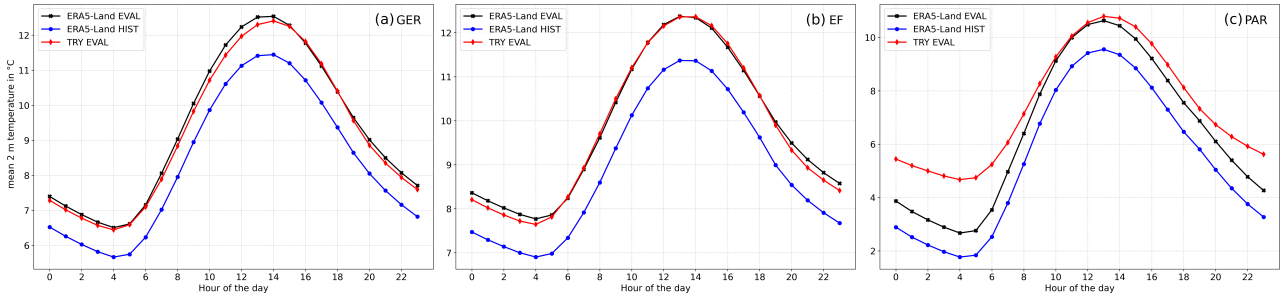

Figure S1. Diurnal cycle of ERA5-Land temperature averaged of the historical reference period 1961–1990 (HIST; blue) and the evaluation period 2005–2014 (EVAL; black) for (a) entire Germany, (b) EF, and (c) PAR. The diurnal cycles of the TRY data for the evaluation period is given in red in each panel. The average diurnal cycles are calculated considering the full year.

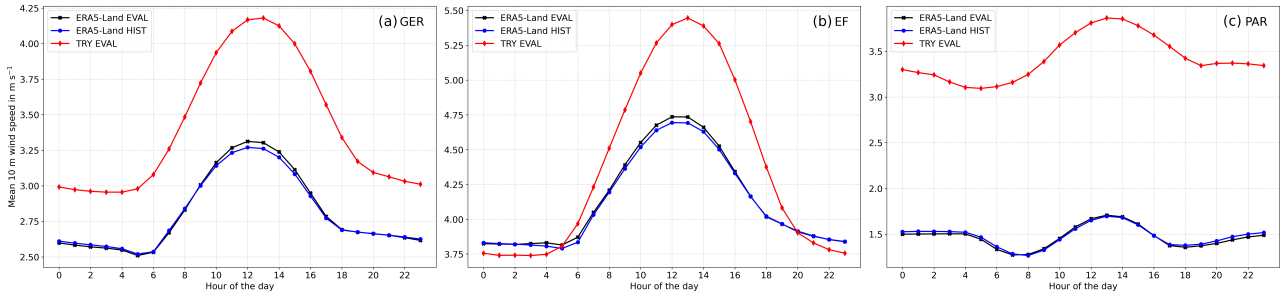

Figure S2. Diurnal cycle of ERA5-Land 10 m wind speed averaged of the historical reference period 1961–1990 (HIST; blue) and the evaluation period 2005–2014 (EVAL; black) for (a) entire Germany, (b) EF, and (c) PAR. The diurnal cycles of the TRY data for the evaluation period is given in red in each panel. The average diurnal cycles are calculated considering the full year.

For the diurnal cycle of wind (Fig. S2), the results reveal some substantial differences between ERA5-Land and TRY. While the course of the diurnal cycle is well captured in ERA5-Land, the absolute values show distinct deviations from TRY depending on the region. For Germany the differences are about 20–30 % throughout the day. The largest deviations are found in the mountainous PAR region, where wind speed in TRY is partly more than twice as high as in ERA5-Land. This could be a result of the rather coarse resolution of ERA5-Land, and hence the inability to capture local wind systems or orographic modifications. The best results can be found in the flat EF region, where the magnitude of wind speed is almost identical during nighttime, and deviations during daytime reach a maximum of 15 %. This could be related to land-sea breeze systems or other local phenomena, which ERA5-Land is not able to capture. The different time periods seem not to play a role as the ERA5-Land data for 1961–1990 is almost identical to the 2005–2014 data. The same characteristics and magnitude of deviations can be found for the annual cycle of wind (Fig. S3).

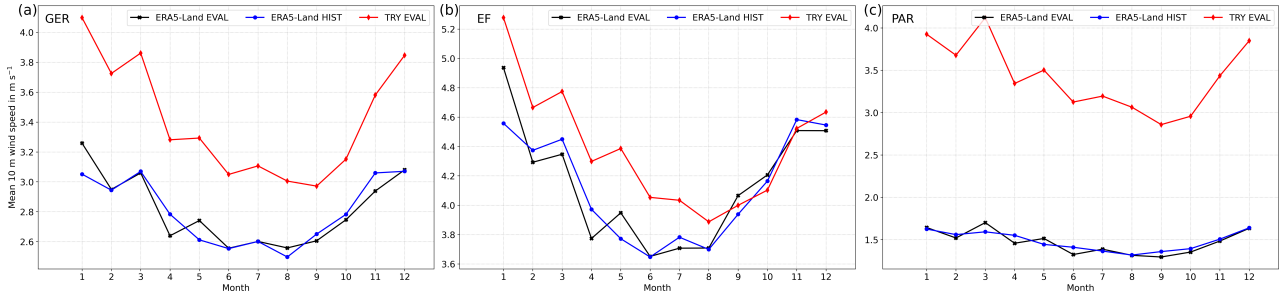

Figure S3. Annual cycle of ERA5-Land 10 m wind speed averaged of the historical reference period 1961–1990 (HIST; blue) and the evaluation period 2005–2014 (EVAL; black) for (a) entire Germany, (b) EF, and (c) PAR. The diurnal cycles of the TRY data for the evaluation period is given in red in each panel.

S2 Analysis of basic meteorological variables

S2.1 Annual and seasonal mean biases

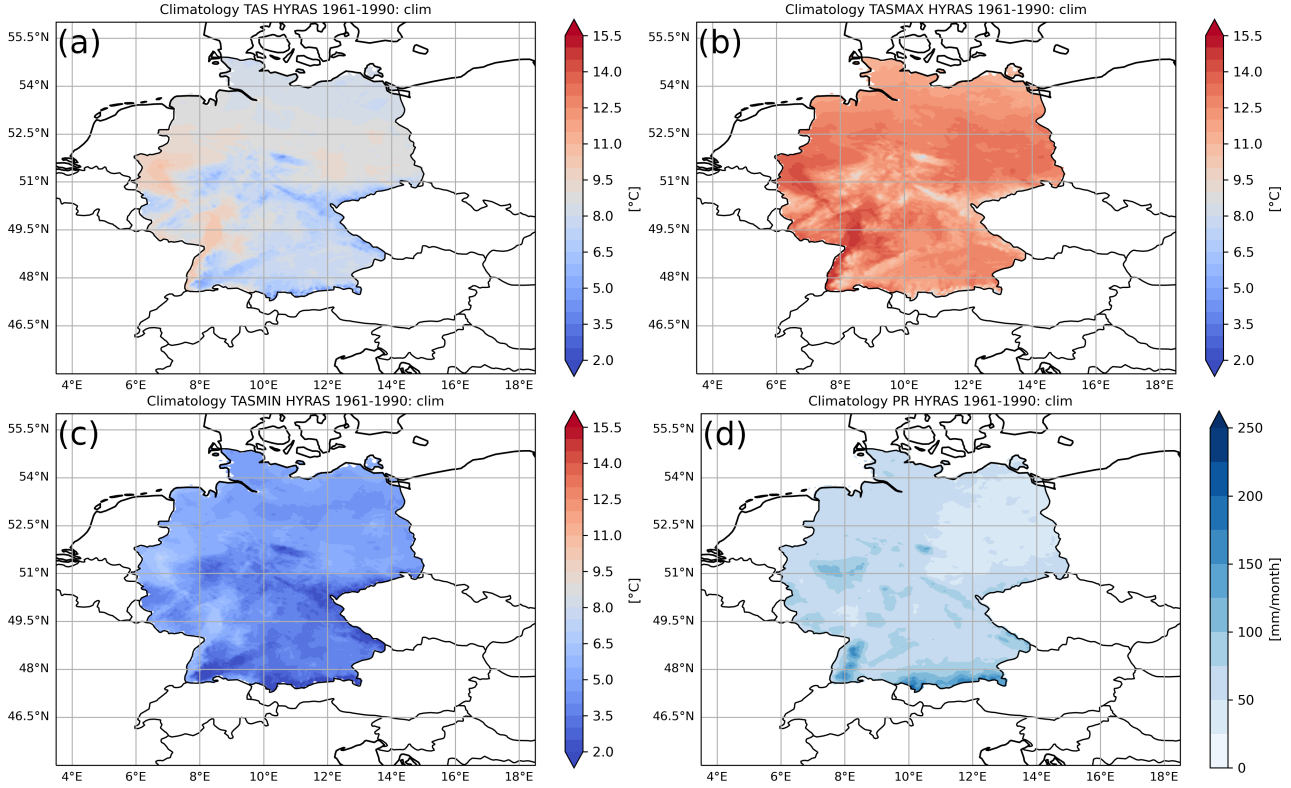

Figure S4. Annual mean of (a) daily mean near-surface air temperature (tas), (b) daily maximum near-surface air temperature (tasmax), (c) daily minimum near-surface air temperature (tasmin), and (d) monthly precipitation sum (pr) for the period 1961–1990 obtained from HYRAS.

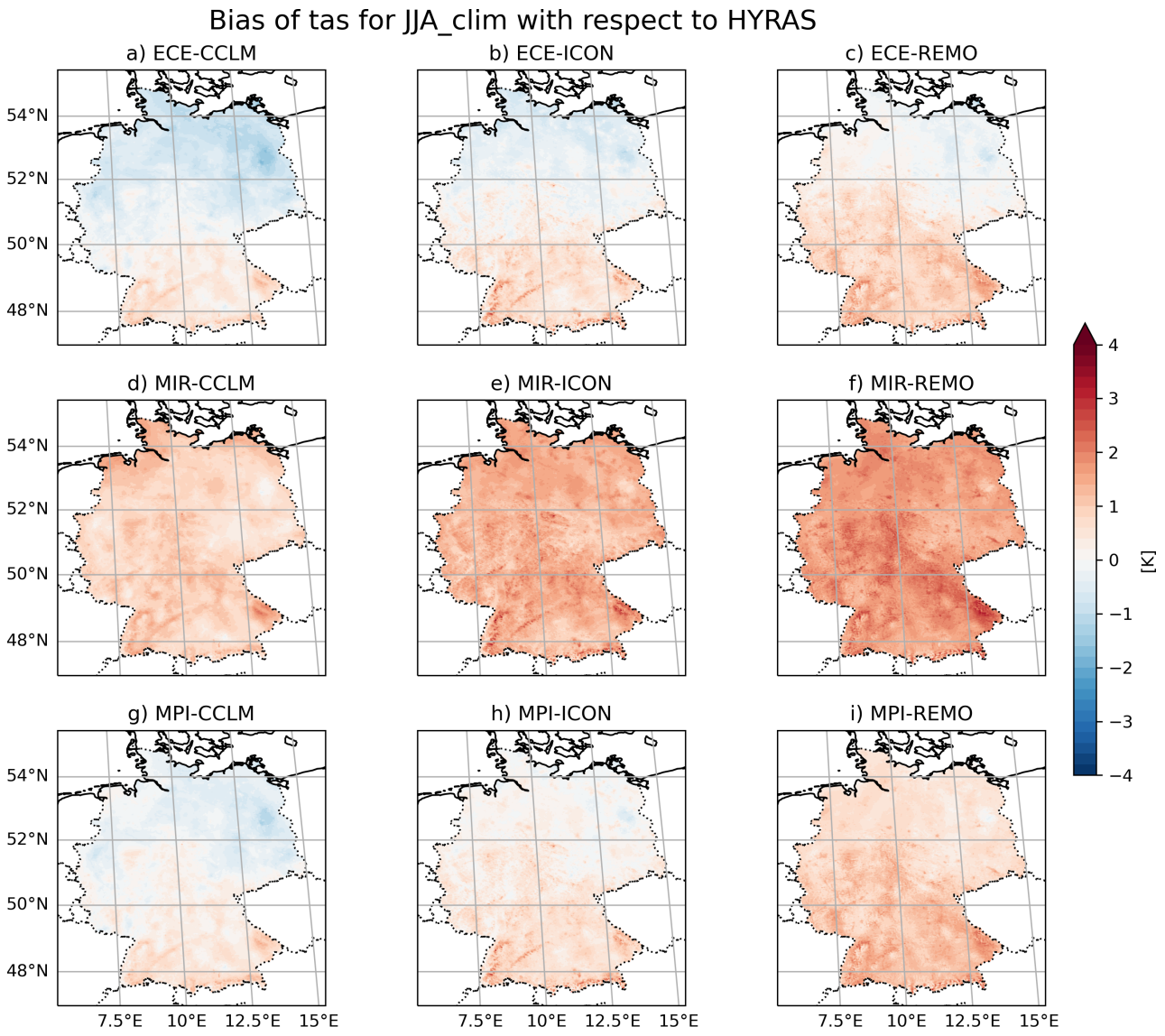

Figure S5. Summer (JJA) seasonal mean bias of near-surface air temperature (tas) simulated by regional climate models against HYRAS.

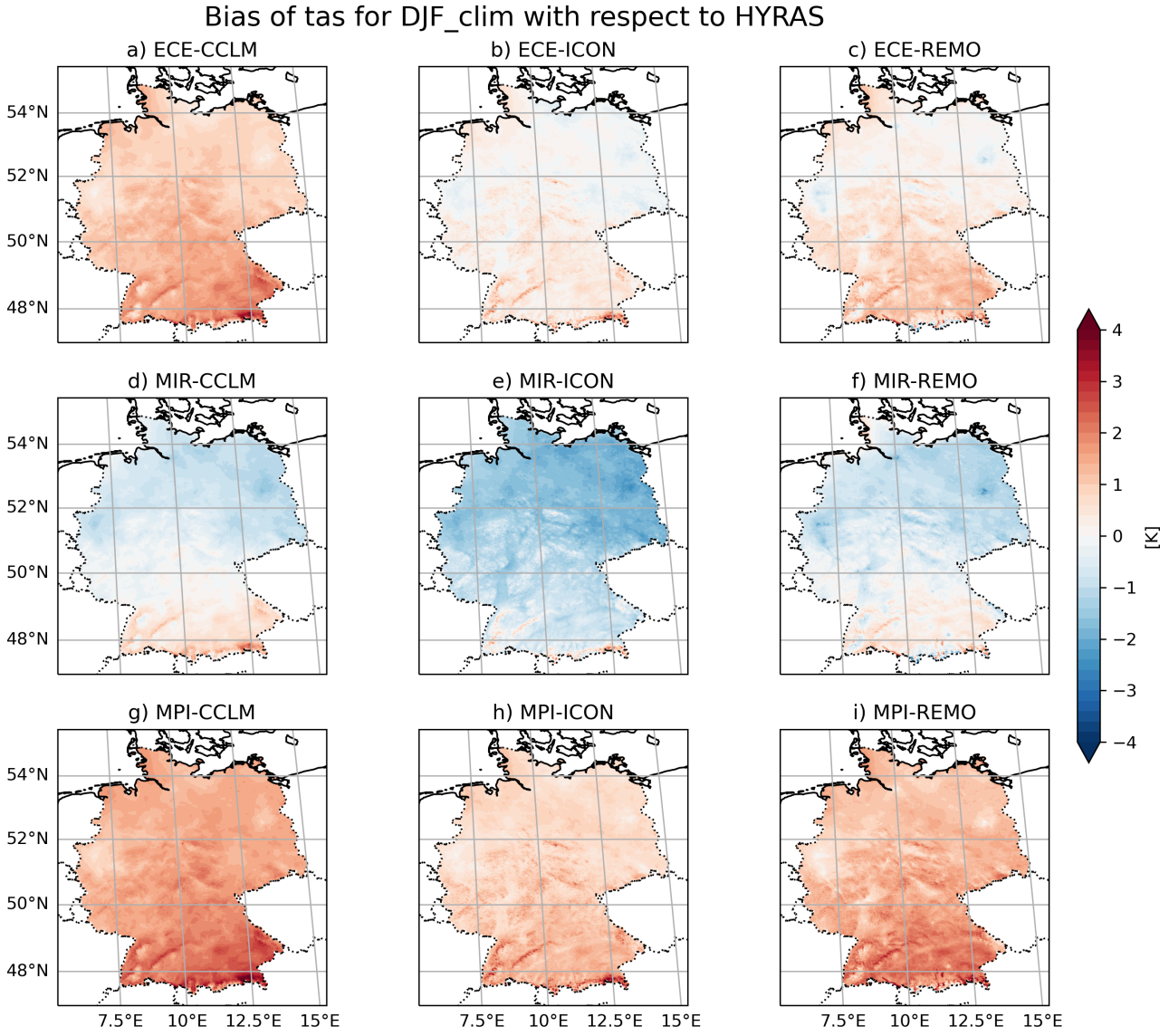

Figure S6. Winter (DJF) seasonal mean bias of near-surface air temperature (tas) simulated by regional climate models against HYRAS.

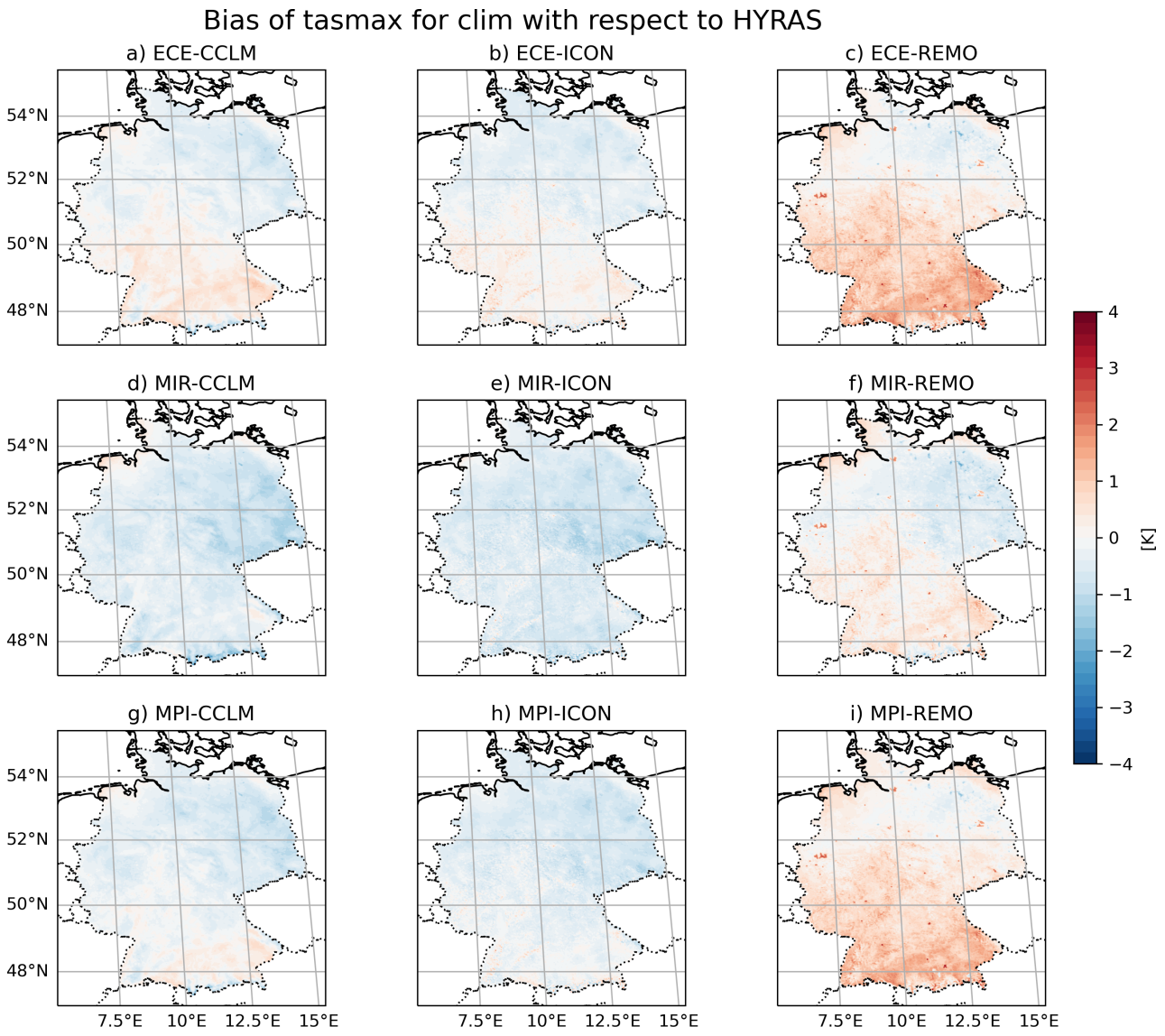

Figure S7. Annual mean bias of daily maximum near-surface air temperature (tasmax) simulated by regional climate models against HYRAS.

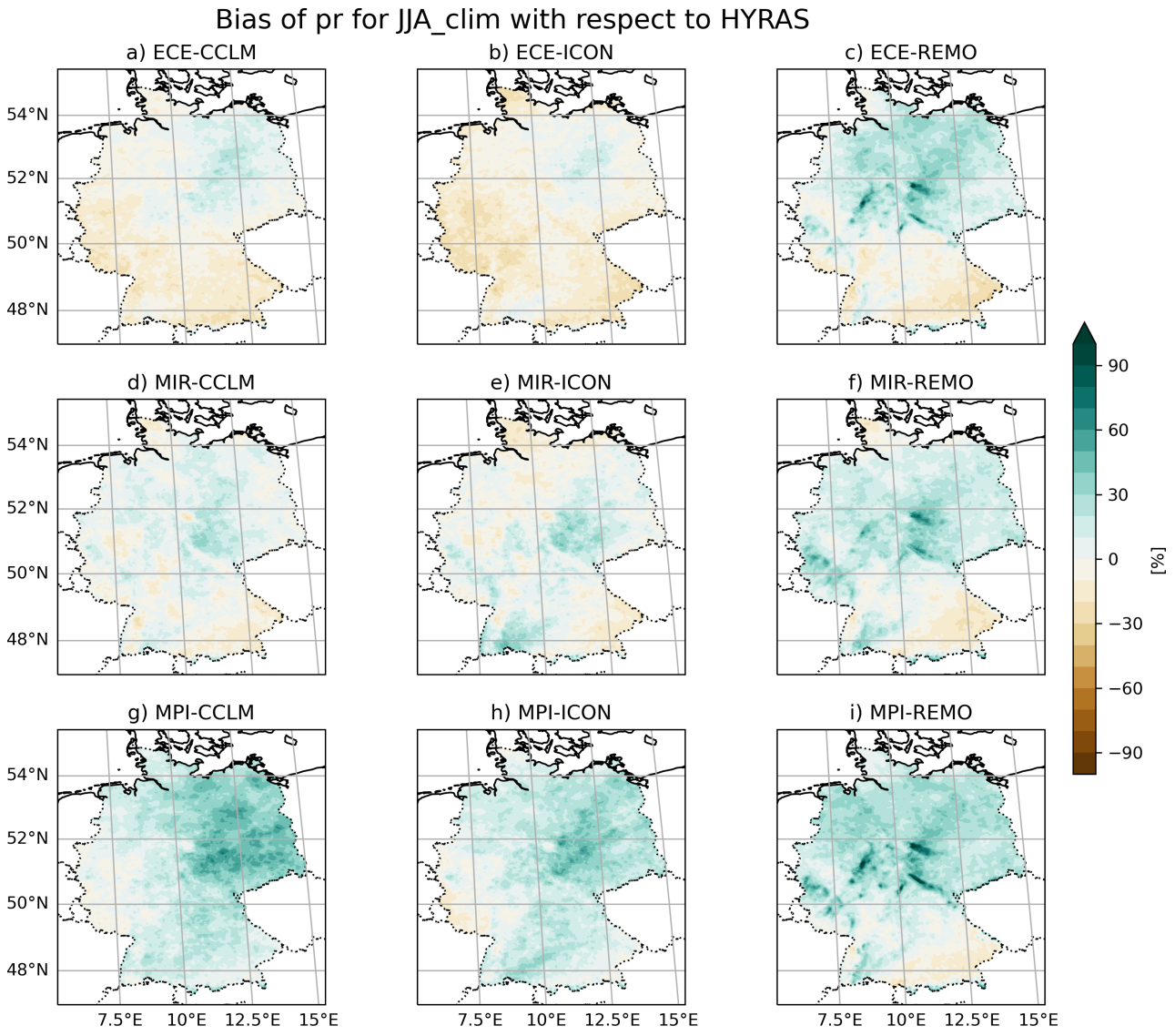

Figure S8. Summer (JJA) relative seasonal mean bias of monthly precipitation sum (pr) simulated by regional climate models against HYRAS.

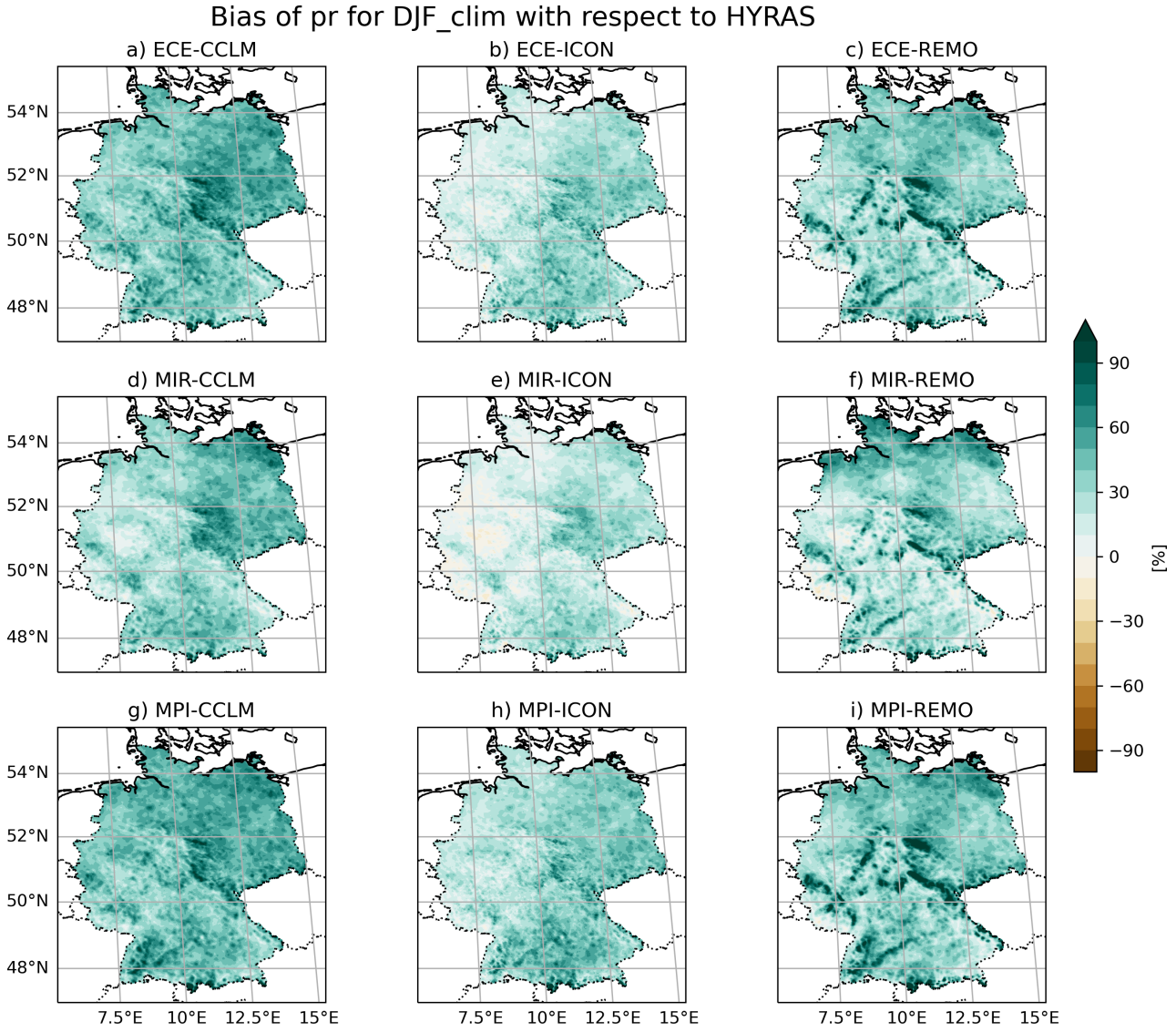

Figure S9. Winter (DJF) relative seasonal mean bias of monthly precipitation sum (pr) simulated by regional climate models against HYRAS.

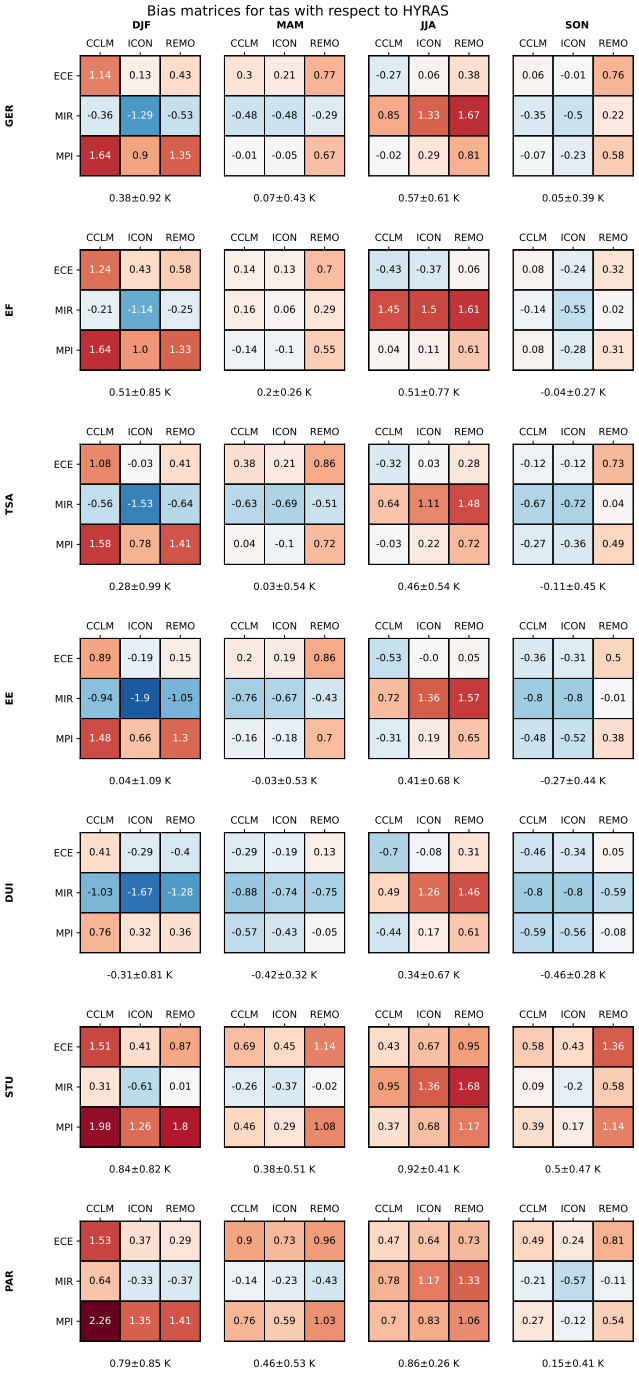

Figure S10. Seasonal mean bias of near-surface air temperature (tas) simulated by regional climate models against HYRAS spatially averaged over NUKLEUS subregions and Germany. The ensemble mean bias for the respective subregion and season is displayed below the corresponding bias matrix with one standard deviation used as measure of uncertainty.

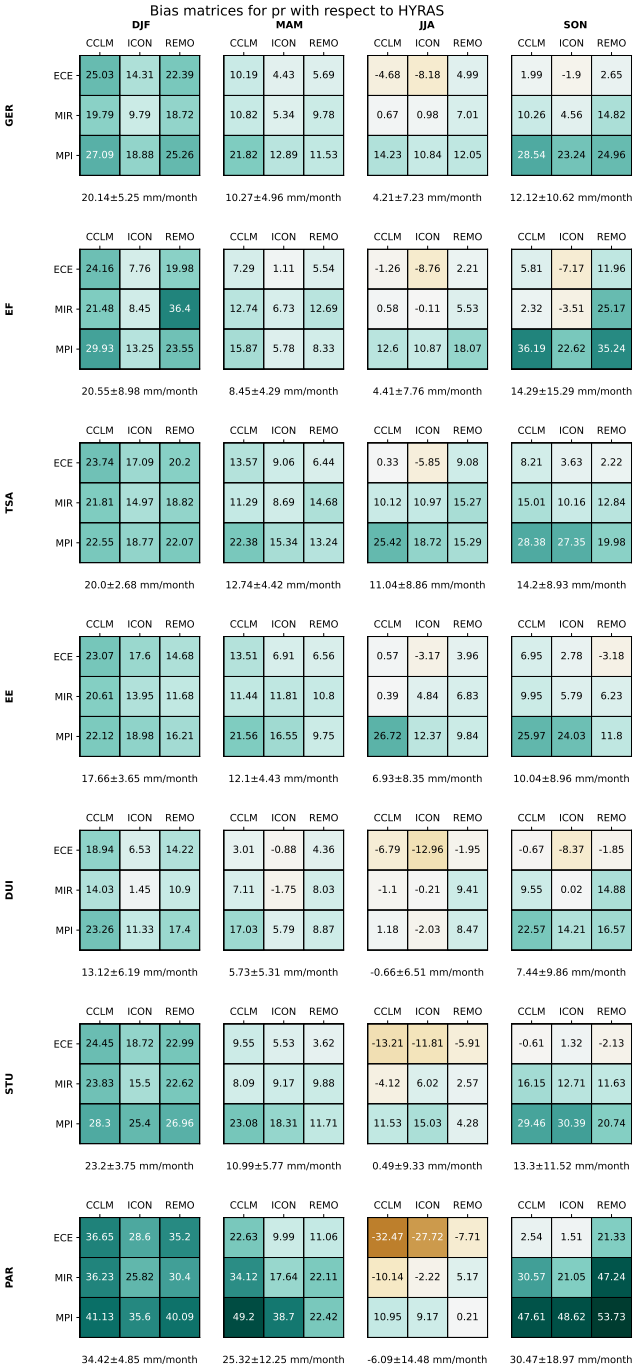

Figure S11. Seasonal mean bias of monthly precipitation sum (pr) simulated by regional climate models against HYRAS spatially averaged over NUKLEUS subregions and Germany. The ensemble mean bias for the respective subregion and season is displayed below the corresponding bias matrix with one standard deviation used as measure of uncertainty.

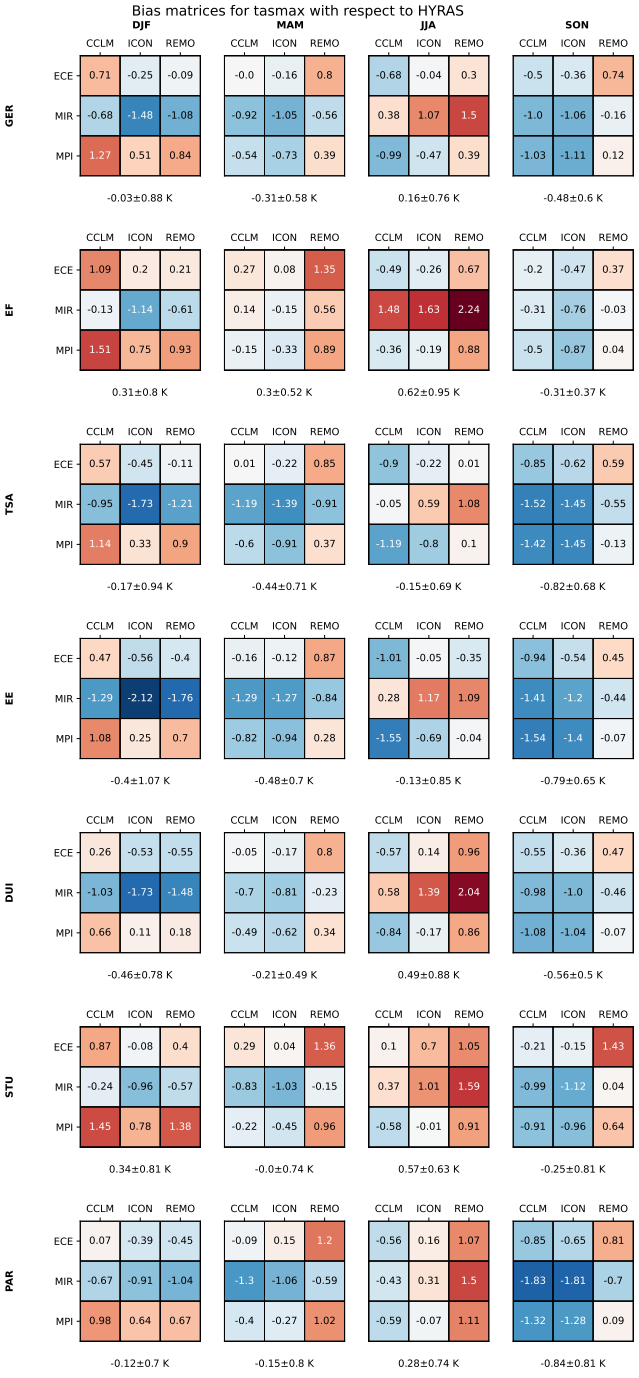

Figure S12. Seasonal mean bias of daily maximum near-surface air temperature (tasmax) simulated by regional climate models against HYRAS spatially averaged over NUKLEUS subregions and Germany. The ensemble mean bias for the respective subregion and season is displayed below the corresponding bias matrix with one standard deviation used as measure of uncertainty.

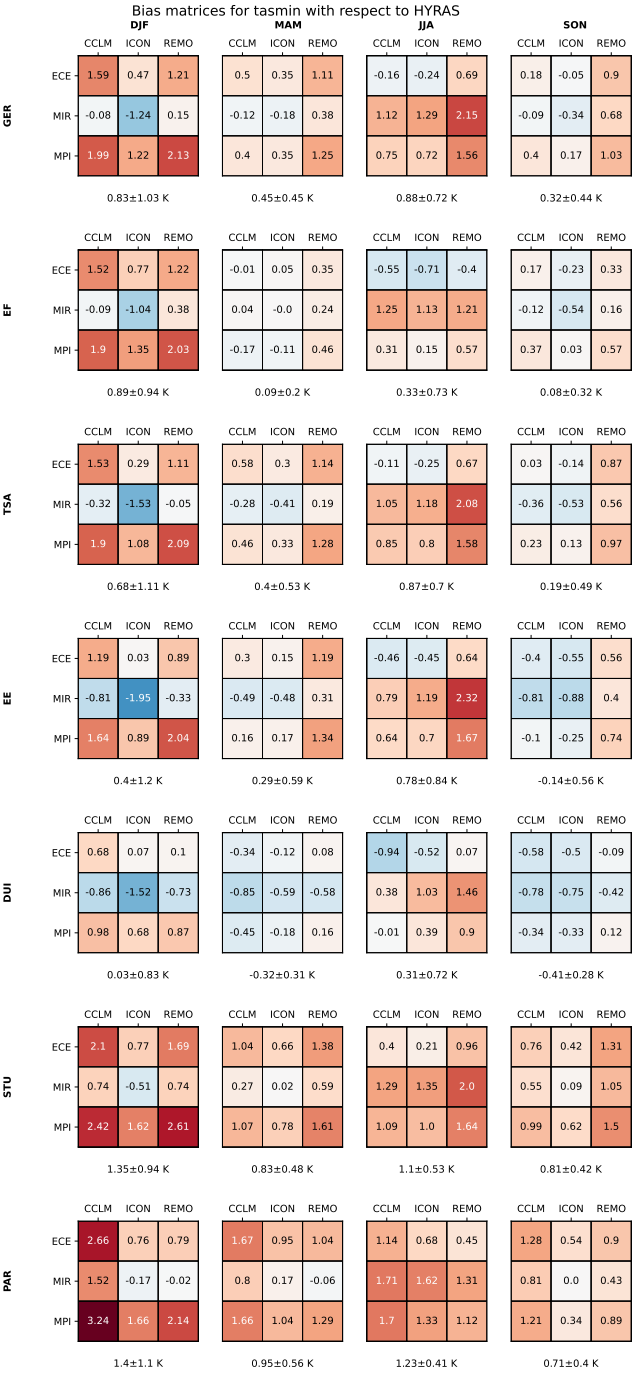

Figure S13. Seasonal mean bias of daily minimum near-surface air temperature (tasmin) simulated by regional climate models against HYRAS spatially averaged over NUKLEUS subregions and Germany. The ensemble mean bias for the respective subregion and season is displayed below the corresponding bias matrix with one standard deviation used as measure of uncertainty.

S2.2 Interannual and interseasonal variability

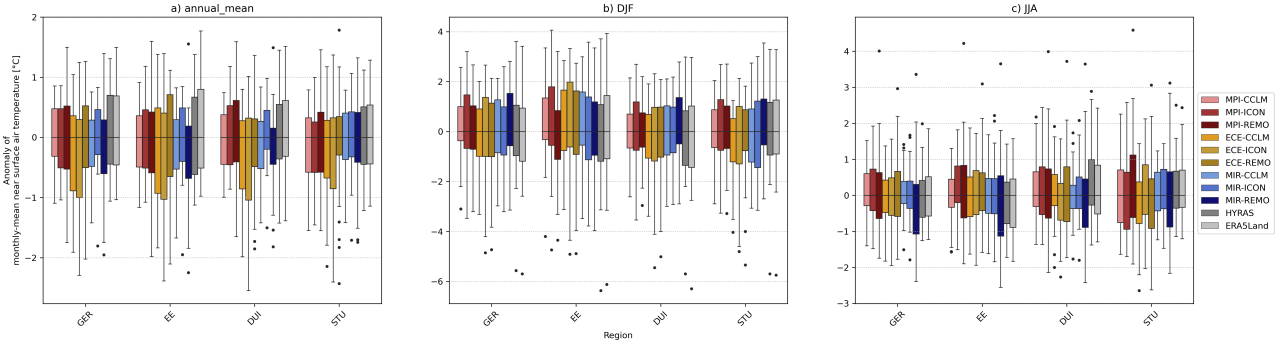

Figure S14. Box plots of median-adjusted annual and seasonal mean 2 m temperature simulated by the RCMs and HYRAS for the pilot regions GER, EE, DUI, and STU, representing the interannual (a) and the interseasonal variability for DJF (b) and JJA (c). To focus on the variability, the median of each model, period, and region was subtracted from the respective data. The center line indicates the median. The box edges represent the interquartile range (IQR). The whiskers mark the farthest point from the nearest box edge within $1.5 \times$ IQR. The dots mark outliers. Note the different scales of the vertical axes.

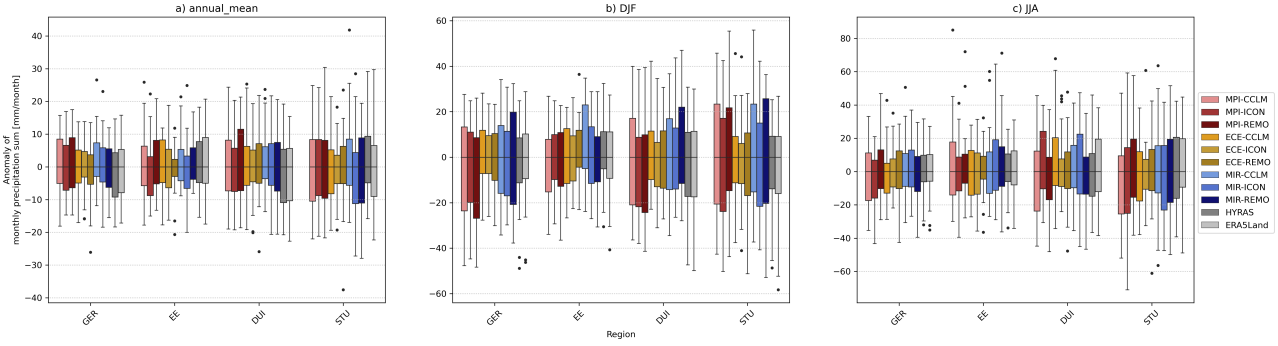

Figure S15. Same as Fig. S14, but for annual and monthly mean (within a season) precipitation totals.

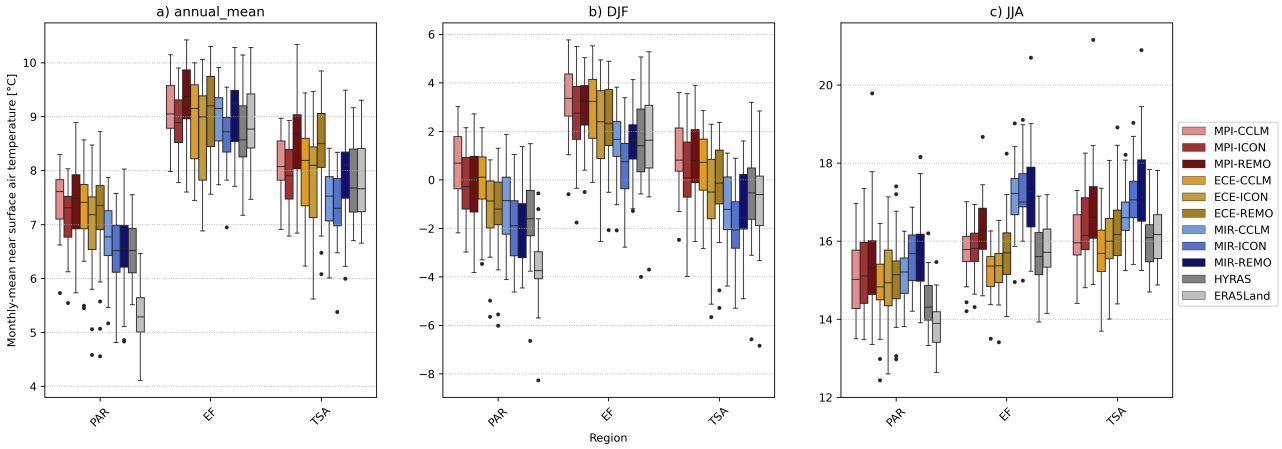

Figure S16. Same as Fig. S14, but for the regions PAR, EF, and TSA, and without subtraction of the median values.

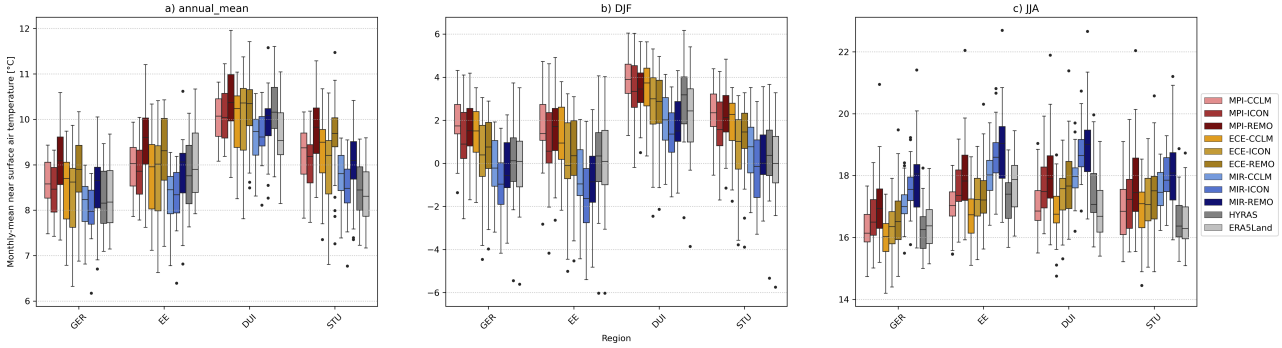

Figure S17. Same as Fig. S14, but without subtraction of the median values.

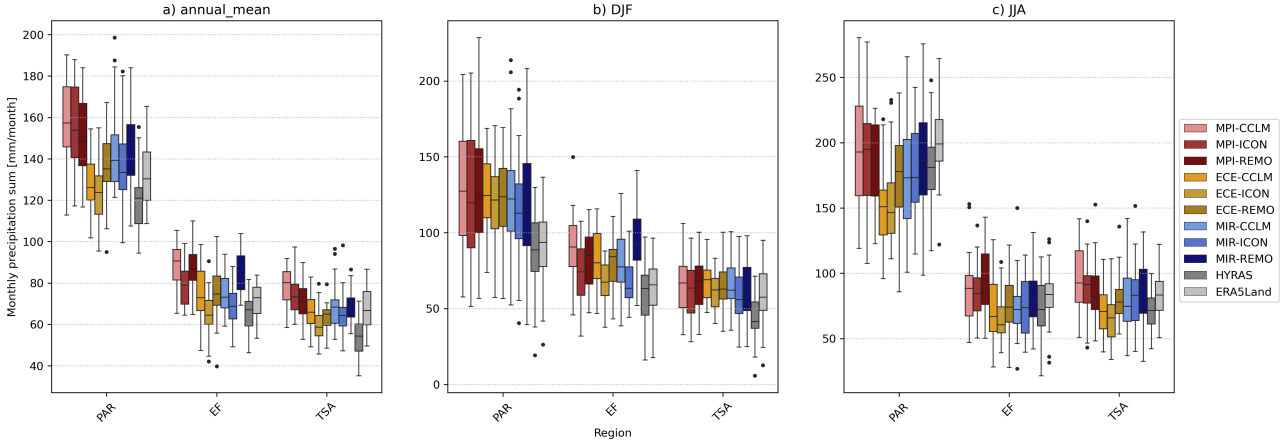

Figure S18. Same as Fig. S14, but for annual and monthly mean (within a season) precipitation totals of the regions PAR, EF, and TSA, and without subtraction of the median values.

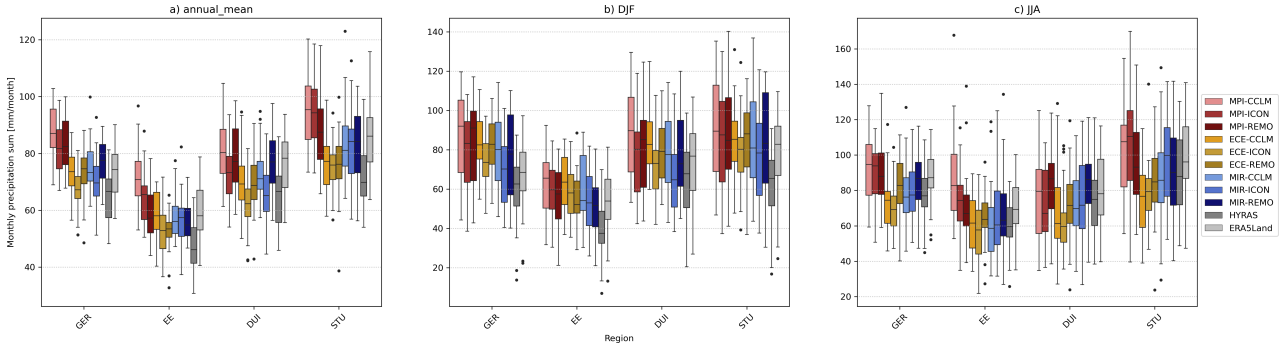

Figure S19. Same as Fig. S14, but for annual and monthly mean (within a season) precipitation totals and without subtraction of the median values.

S2.3 Annual cycles

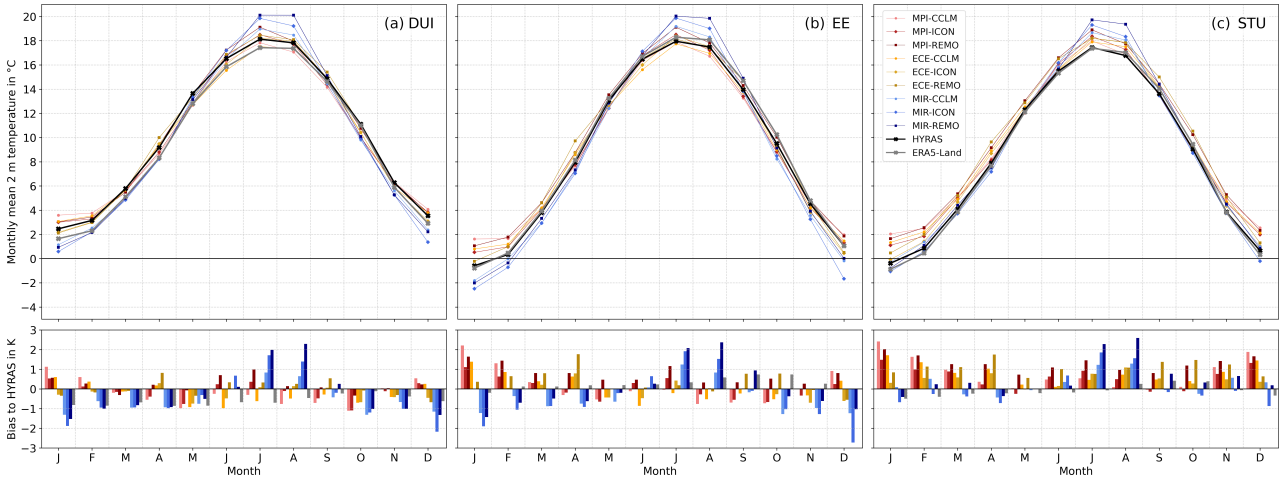

Figure S20. Annual cycle of monthly mean 2 m temperature for the pilot region of (a) DUI, (b) EE, and (c) STU for HYRAS (black, crosses), ERA5-Land (gray, crosses), and the NUKLEUS ensemble: reddish colors mark the CPM simulations driven by MPI-ESM (MPI), yellowish colors those driven by EC-Earth (ECE), and blueish those driven by MIROC6 (MIR); dots indicate the COSMO-CLM simulations (CCLM), diamonds the ICON-CLM simulations (ICON), and squares the REMO simulations. The bar plot at the bottom gives the bias towards HYRAS of all simulations and ERA5-Land.

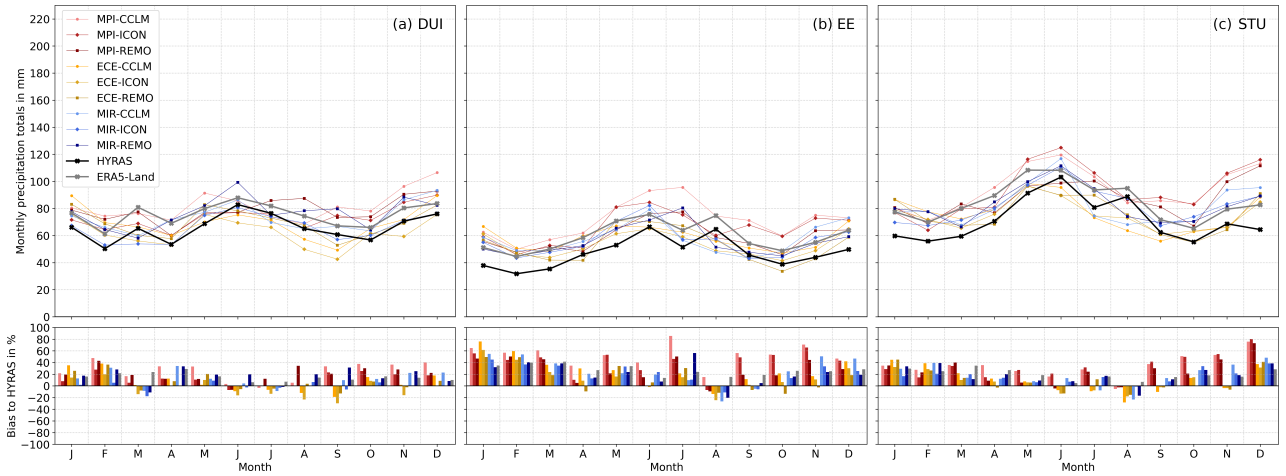

Figure S21. Same as Fig. S20, but for monthly precipitation totals.

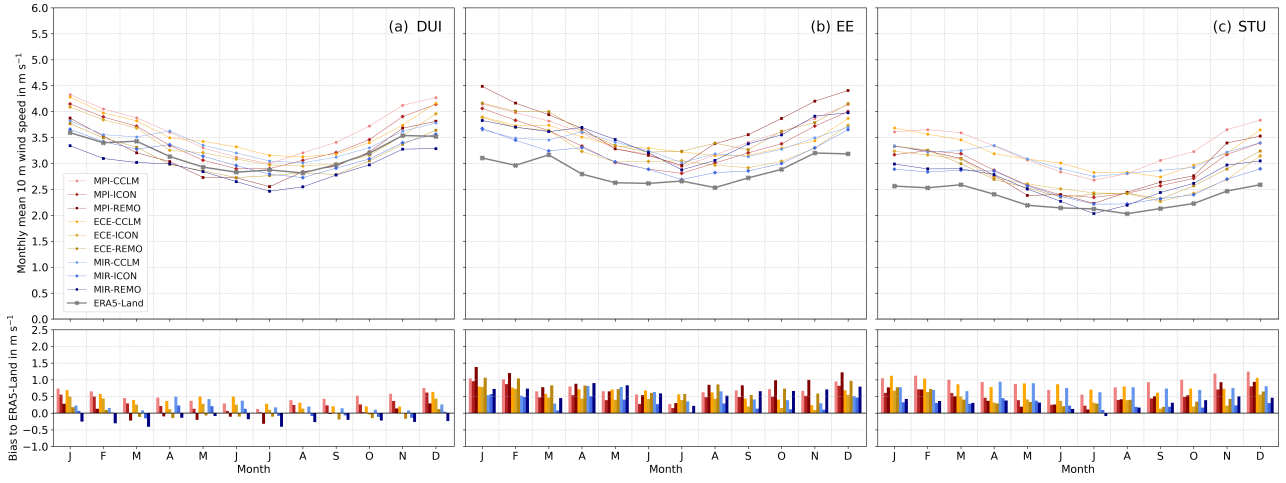

Figure S22. Same as Fig. S20, but for monthly mean 10 m wind speed. Note that there is no wind data in HYRAS, and, therefore, the bias is calculated towards ERA5-Land.

S2.4 Frequency distributions

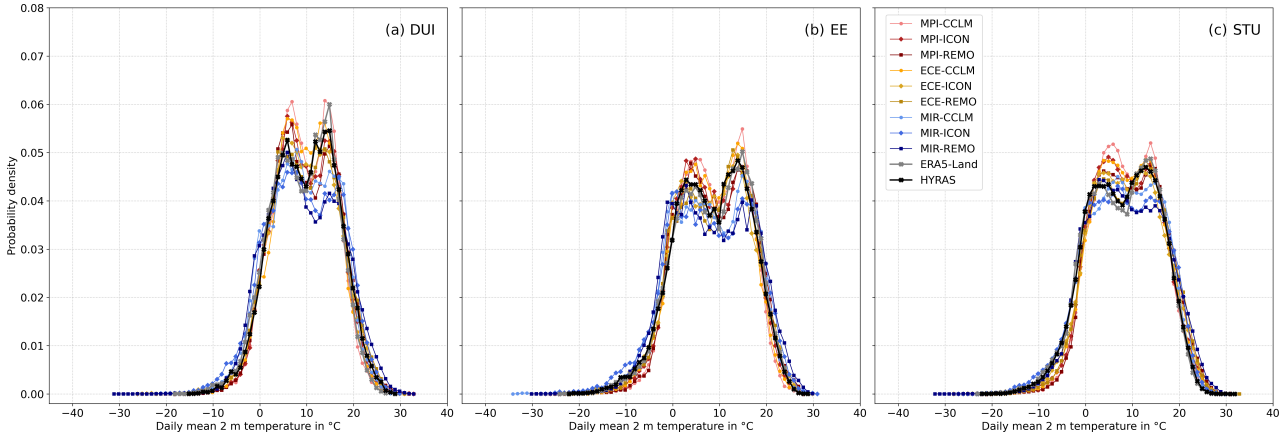

Figure S23. Frequency distribution of daily mean 2 m temperature (Tmean), taking into account every single grid point within the pilot region of (a) DUI, (b) EE, and (c) STU for HYRAS (black, crosses), ERA5-Land (gray, crosses), and the NUKLEUS ensemble: reddish colors mark the CPM simulations driven by MPI-ESM (MPI), yellowish colors those driven by EC-Earth (ECE), and blueish those driven by MIROC6 (MIR); dots indicate the COSMO-CLM simulations (CCLM), diamonds the ICON-CLM simulations (ICON), and squares the REMO simulations.

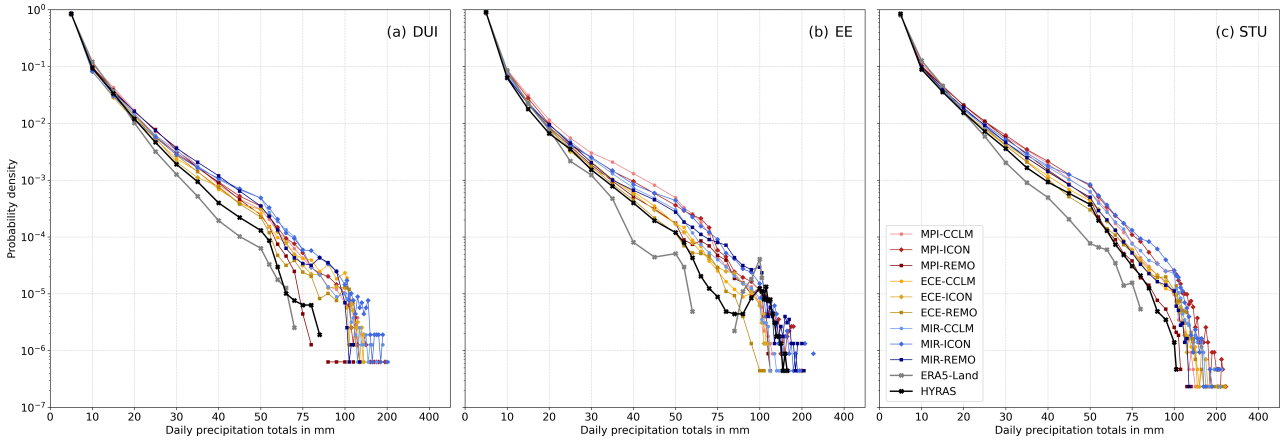

Figure S24. Same as Fig. S20, but for daily precipitation totals. Please note the non-linear x-axis.

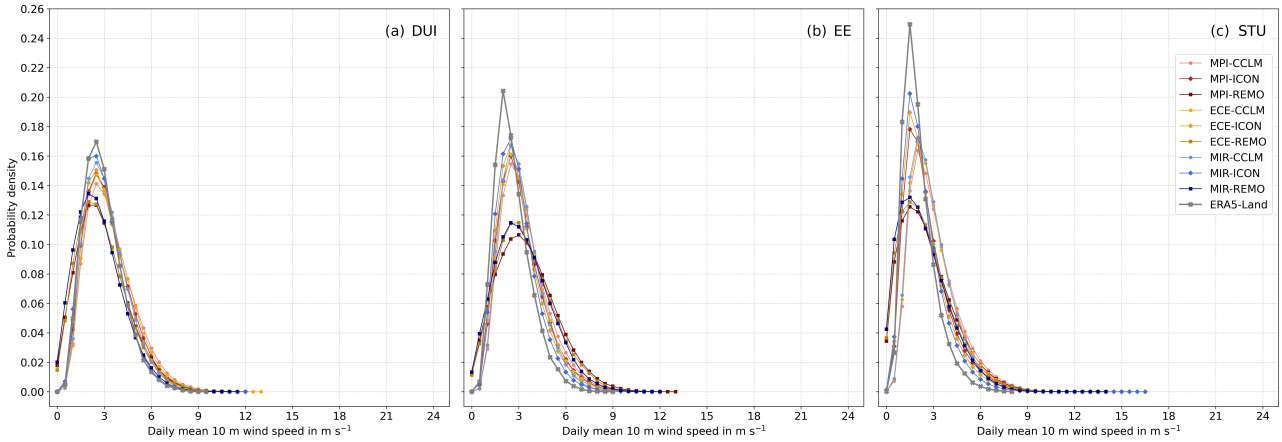

Figure S25. Same as Fig. S20, but for daily mean 10 m wind speed. Note that there is no wind data in HYRAS.

Table S1. Perkins skill score (PSS) using HYRAS as reference data set for daily mean 2 m temperature and daily precipitation totals, and ERA5-Land as reference for daily mean 10 m wind speed in the pilot regions DUI, EE, and STU for all members of the NUKLEUS ensemble. PSS ≥ 0.95 are marked **in bold**, $0.90 \leq$ PSS < 0.95 are marked *in italics*. Note that due to rounding to two decimal places, the same rounded PSS can be marked with both types.

Model	2 m temperature			Precipitation			10 m wind speed		
	DUI	EE	STU	DUI	EE	STU	DUI	EE	STU
MPI-CCLM	*0.93*	*0.93*	*0.93*	**0.96**	*0.95*	**0.95**	0.87	0.79	0.71
MPI-ICON	**0.95**	**0.96**	*0.95*	**0.99**	**0.96**	**0.96**	*0.93*	0.84	0.84
MPI-REMO	**0.96**	*0.94*	*0.93*	**0.98**	**0.98**	**0.97**	0.86	0.70	0.72
ECE-CCLM	*0.94*	**0.95**	*0.94*	**0.99**	**0.97**	**0.99**	0.89	0.82	0.73
ECE-ICON	**0.97**	**0.96**	**0.95**	**0.98**	**0.98**	**1.00**	*0.94*	0.87	0.87
ECE-REMO	**0.97**	**0.96**	**0.95**	**0.99**	**0.99**	**0.99**	0.87	0.73	0.73
MIR-CCLM	*0.93*	*0.93*	**0.96**	**0.99**	**0.98**	**0.98**	*0.93*	0.83	0.74
MIR-ICON	*0.91*	*0.91*	*0.94*	**0.98**	**0.99**	**0.99**	**0.98**	*0.90*	0.90
MIR-REMO	*0.91*	0.89	*0.93*	**0.99**	**0.99**	**0.98**	0.86	0.74	0.74

S2.5 Diurnal cycles

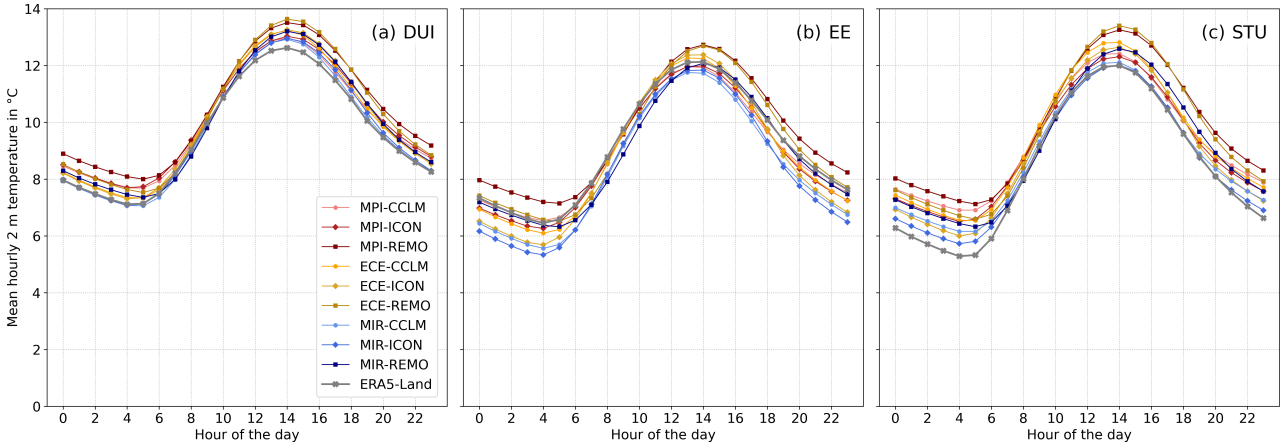

Figure S26. Diurnal cycle of mean hourly 2 m temperature for the pilot region of (a) DUI, (b) EE, and (c) STU for ERA5-Land (gray, crosses), and the NUKLEUS ensemble: reddish colors mark the CPM simulations driven by MPI-ESM (MPI), yellowish colors those driven by EC-Earth (ECE), and blueish those driven by MIROC6 (MIR); dots indicate the COSMO-CLM simulations (CCLM), diamonds the ICON-CLM simulations (ICON), and squares the REMO simulations.

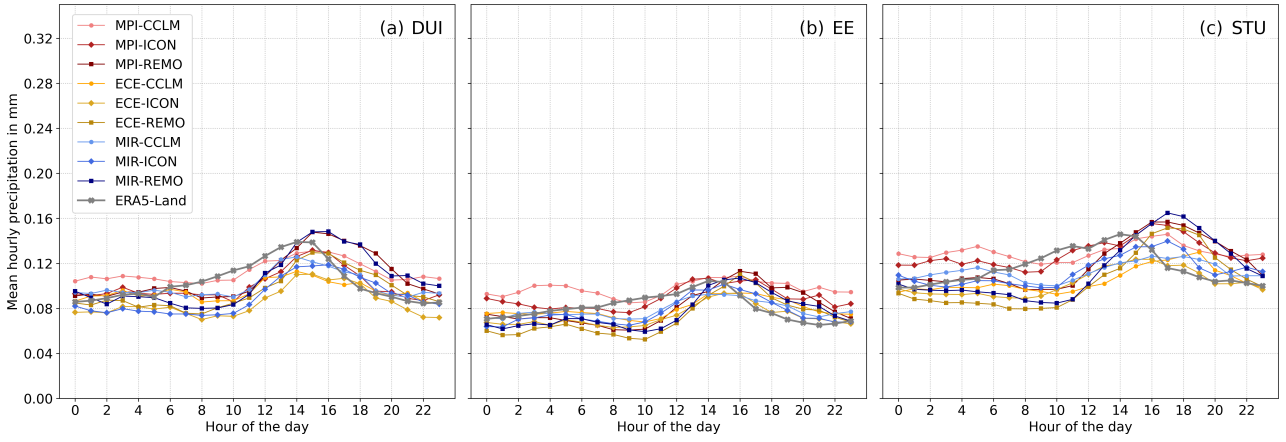

Figure S27. Same as Fig. S20, but for mean hourly precipitation.

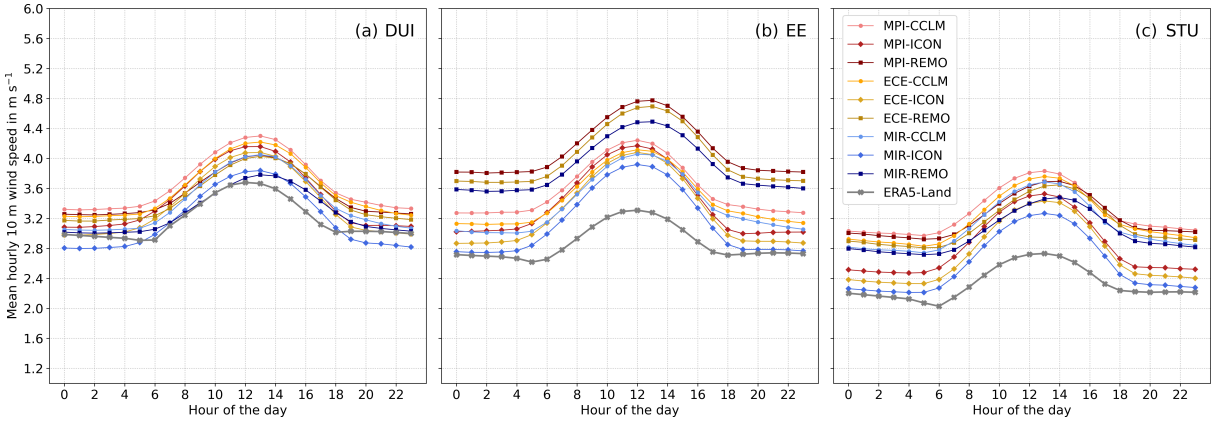

Figure S28. Same as Fig. S20, but for mean hourly 10 m wind speed. Note that there is no wind data in HYRAS available.

S3 Climate indices

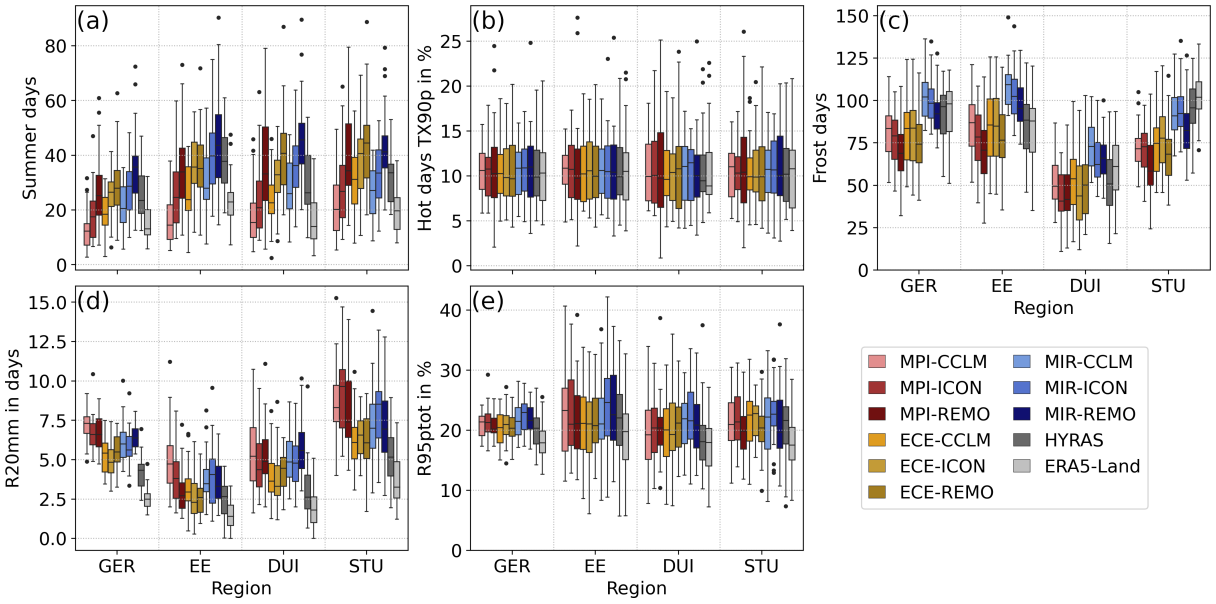

Figure S29. Box plots of the selected climate indices of the annual number of (a) summer days, (b) hot days with temperatures above the 90th percentile (TX90p), (c) frost days, (d) very heavy rain days with daily totals above 20 mm (R20mm), and (e) the contribution of very wet days with daily totals above the 95th percentile to the total annual precipitation (R95ptot) for entire Germany (GER), and the pilot regions DUI, EE, and STU for the period 1961–1990 for HYRAS (dark gray), ERA5-Land (light gray), and the NUKLEUS ensemble: reddish colors mark the CPM simulations driven by MPI-ESM (MPI), yellowish colors those driven by EC-Earth (ECE), and blueish those driven by MIROC6 (MIR). The center line indicates the median, the box edges the interquartile range (IQR), and the whiskers extend to 1.5 × IQR. The dots mark outliers.

S4 Bias-corrected NUKLEUS data

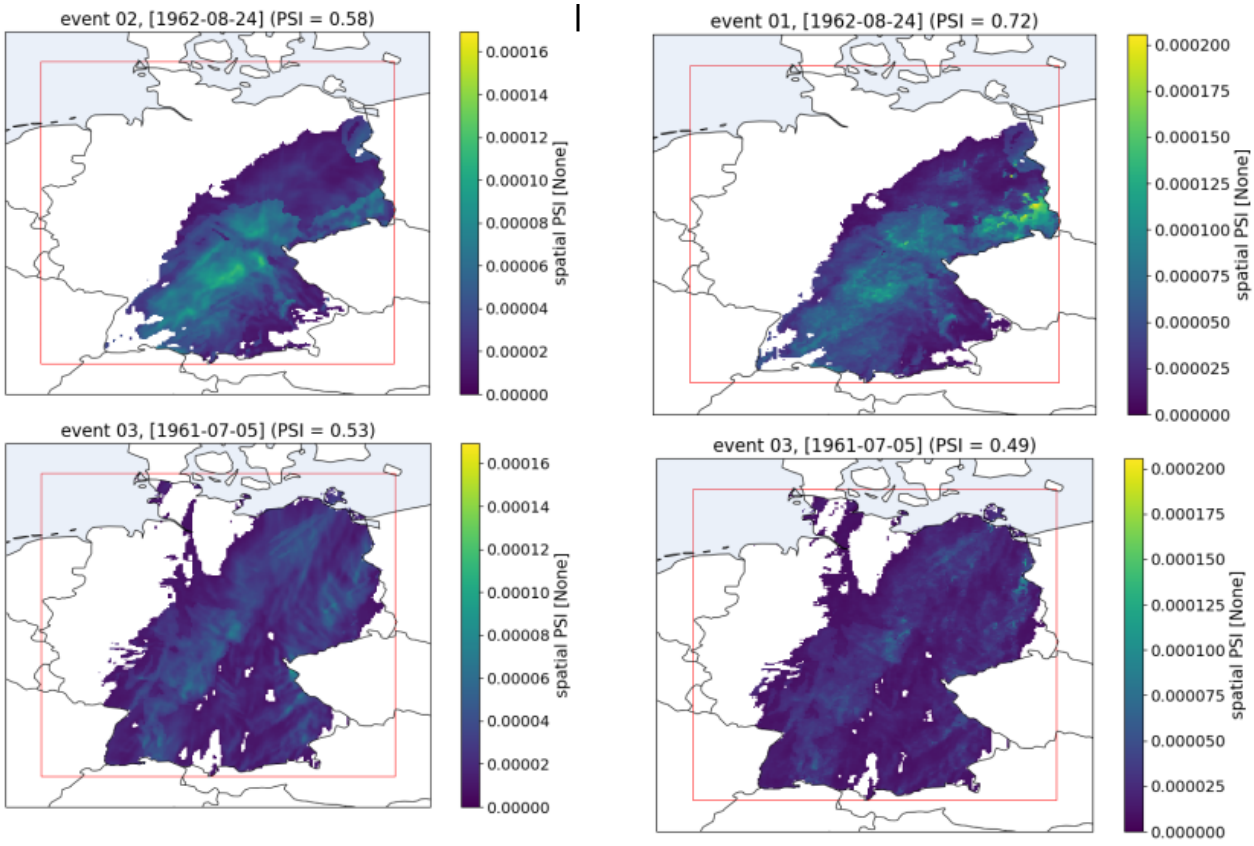

Figure S30. Spatial distribution of precipitation severity index (PSI) for the second and third most extreme precipitation events detected in the original data of the simulation conducted with EC-Earth driven COSMO-CLM (left). Corresponding precipitation events detected in the bias corrected data of the same simulation (right). In the bias corrected data these events are ranked as the first and third most extreme precipitation events.

References

Deutscher Wetterdienst, 2026: Klimastatusbericht Deutschland Jahr 2025, DWD, Geschäftsbereich Klima und Umwelt, Offenbach am Main, 30 pp., ISSN 1616–5063, available at: https://www.dwd.de/DE/leistungen/klimastatusbericht/klimastatusbericht.html.

Krähenmann, S., Walter, A., Brienen, S., Imbery, F., and Matzarakis, A., 2016: Monthly, daily and hourly grids of 12 commonly used meteorological variables for Germany estimated by the project TRY advancement, https://doi.org/10.5676/DWD_CDC/TRY_BASIS_V001.